# Self-diffusion in inhomogeneous granular shearing flows

Riccardo Artoni [*] and Patrick Richard

MAST-GPEM, Université Gustave Eiffel, IFSTTAR, F-44344 Bouguenais, France

Michele Larcher

Free University of Bozen-Bolzano, I-39100 Bozen-Bolzano, Italy

James T. Jenkins

Cornell University, Ithaca, New York 14053, USA

In this Letter, we discuss how flow inhomogeneity affects the self-diffusion behavior in granular flows. Whereas self-diffusion scalings have been well characterized in the past for homogeneous shearing, the effect of shear localization and nonlocality of the flow has not been studied. We, therefore, present measurements of self-diffusion coefficients in discrete numerical simulations of steady, inhomogeneous, and collisional shearing flows of nearly identical, frictional, and inelastic spheres. We focus on a wide range of dense solid volume fractions, that correspond to geophysical and industrial shearing flows that are dominated by collisional interactions. We compare the measured values first with a scaling based on shear rate and, then, on a scaling based on the granular temperature. We find that the latter does much better than the former in collapsing the data. The results lay the foundations of diffusion models for inhomogeneous shearing flows, which should be useful in treating problems of mixing and segregation.

Introduction. Diffusion is a key mechanism for mass transfer in granular shearing flows. In such flows, collisions between spheres induce velocity fluctuations of the grains that drive the motion of particles in a way that is analogous to the thermal diffusion in dense gases, or the dispersion induced by eddies in turbulent flows. Such shear-induced diffusion is important for applications in industrial and natural granular flows involving mixing and segregation. The problems encountered share many features with other research involved with transport phenomena and motion of discrete bodies, and, therefore, advances in the comprehension of diffusion are profitable to several soft matter fields (granular materials, suspensions, traffic, and crowd dynamics, active matter,...). Experimental and numerical studies have been devoted to characterize diffusion in various flow geometries, often in connection with segregation: granular shear cells or simple shear flows [1–3]; vertical channels [4,5]; inclined chutes [6]; rotating drums [7,8]. Phenomenological theories of segregation during flow [9,10], that produce plausible predictions of species' concentrations and mixture velocity for appropriate choices of parameters, generally involve simple models for the mechanism of diffusion.

Despite the amount of studies, few have addressed in detail the anisotropic nature of self-diffusion and its scaling with the relevant kinematic parameters. For dilute systems (solid fraction lower than 0.5), Campbell [11] measured the self-diffusivity tensor by means of numerical simulations of a homogeneously sheared system of frictional inelastic spheres. Utter and Behringer [12] performed experiments on slow, rate-independent, and inhomogeneous shearing of a dense aggregate of disks in a Couette cell, pointing to the existence of anisotropy and showing that in the dense limit, self-diffusion coefficients scale approximately as $D = k d^2 \dot{\gamma}$, where $\dot{\gamma}$ is the shear rate, and d is the particle diameter. It was later shown that in three dimensions, k is a constant on the order of 0.05 [13–15]. More recently, we [13] extended Campbell's work by numerically studying dense systems (solid volume fraction in the range of 0.49 to 0.587) under homogeneous shear, characterizing the full self-diffusion tensor and discussing different scalings for the transverse diffusivity. For the same simplified flow configuration, Macaulay and Rognon [16] investigated the effect of intergranular cohesive forces on diffusion.

Nearly all these studies dealt with homogeneous shearing. Inhomogeneous shearing flows are obviously more complex. In regions of shear localization and creep, and those influenced by boundaries [17], the rheology is known to become nonlocal, which means that the local effective friction is not simply determined by a balance between shear and confinement. In analogy with molecular theories, the introduction of velocity fluctuations as an additional variable seems a promising path. The strength of velocity fluctuations is a classical ingredient of diffusion theories, and dense kinetic theories for the segregation of binary mixtures of inelastic spheres [18–22] predict diffusion coefficients that exhibit explicit dependence on the volume fraction, the strength of the particle velocity fluctuations, and the particles' size, mass, and collision properties. The important question we address here in detail is how

———————
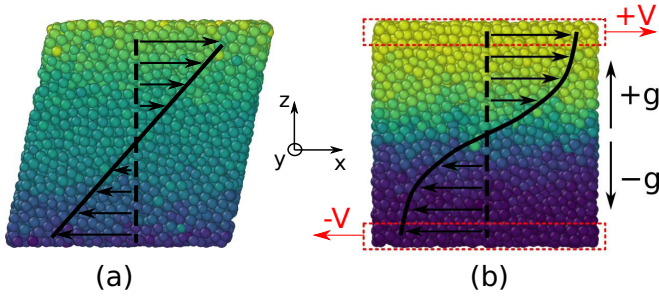*[*]riccardo.artoni@univ-eiffel.fr

FIG. 1. The two flow configurations studied in this Letter: (a) homogeneous shear flow and (b) concave flow. Cell height is $20d$. The lighter yellow corresponds to the largest velocity to the right, and the darker blue corresponds to the largest velocity to the left.

the inhomogeneity of the flow affects self-diffusion, and, in particular, whether the scaling of diffusivity on shear rate has to be replaced by one based on granular temperature, inspired by kinetic theory [13].

Here, we focus on flows in the range of volume fractions between 0.35 and 0.6. This comprises the range of volume fraction important in geophysical flows on Earth. Above a volume fraction of 0.49, long range order can appear in an equilibrated system of identical elastic spheres [23], and at a volume fraction of about $\phi_c = 0.587$, collisional flow becomes impossible, when the coefficient of sliding friction is 0.5 [24]. In order to address the question raised above, we measure the components of self-diffusion parallel and perpendicular to the flow in discrete numerical simulations of inelastic spheres in dense, steady, and inhomogeneous shearing flows. We test the scaling based on the shear rate with that based on the granular temperature and determine that the kinetic theory scaling does far better than the shear rate scaling in collapsing the data for inhomogeneous flows over a range of very dense volume fractions and strength of inhomogeneity.

Flow configurations. Discrete element method simulations were performed by means of the open source LAMMPS platform [25]. The numerical samples were slightly polydisperse, characterized by uniform (number-based) particle size distribution in the range of $0.9d$–$1.1d$, where d is the characteristic particle diameter. Masses were nondimensionalized with respect to the mass m of a particle with size d (in practice, this corresponds to take a normalized density of $6/\pi$). Simulations were performed in a cuboidal fixed volume cell ($L = 20d$). A classical linear spring-dashpot model with tangential elasticity and friction was chosen as a contact model. The viscous damping coefficient was adjusted to yield a normal coefficient of restitution $e_n = 0.7$, and the interparticle friction coefficient was taken equal to $\mu = 0.5$. Tangential stiffness was taken proportional to the normal one $k_t/k_n = 2/7$; a classical assumption which ensures that the period of tangential oscillations is the same as the period of normal oscillations after a contact.

Results from two types of flows (displayed in Fig. 1) are presented in the following. The flows are steady, fully developed, and quasibidimensional. For flow configurations, we identify x as the flow, or streamwise, direction, z as the direction in which we impose a velocity gradient, and y as the

transverse direction. In terms of the mean velocity field $\vec{v} = [v_x(z), 0, 0]$, the first configuration is homogeneous shearing without gravity, which was the subject of a previous work [13], and which is taken here as the reference case. Homogeneous shear was obtained by means of fully periodic boundary conditions coupled with continuous domain deformation as in LAMMPS's "fix deform" scheme. The solid fraction was varied in the range of 0.49–0.587 in this configuration. Given that the volume was fixed, this was simply obtained by tuning the number of particles N. The second configuration may be referred to—after the shape of the shearing profile—as a concave flow [26]. The shearing profile results from a nontrivial pattern of external forces given by $F_z = mg\frac{z-z_0}{|z-z_0|}$ where z_0 is the midpoint of the system. The shearing takes place at constant volume by imposing the velocity ($\pm V$) of two layers at the extremes of the cell in the z direction, each layer being $2d$ thick (the effective flow height being, therefore, $H = 16d$). Periodic boundary conditions hold in the other directions. In practice, the global shear rate (i.e., $2V/H$) was kept constant, and the gravitational acceleration g was varied in order to vary the z heterogeneity of the system. The initial state of the system was extracted from homogeneous shear tests at three different global solid fractions ($\phi \approx 0.53, 0.55, 0.57$).

The systems studied possess three time scales: one related to contact stiffness $\tau_s = \sqrt{m/k_n}$, one related to shearing $\tau_\gamma = 1/\dot{\gamma}$, and one related to pressure $\tau_p = d/\sqrt{p/\rho}$. The latter, τ_p and τ_γ have to be much larger than the former τ_s to keep the particle contacts sufficiently rigid. This guided the choice of the shear rate, which was chosen in order to ensure $\tau_\gamma \sim 10^3 \tau_s$ locally for the homogeneous shear, and globally for the concave flow simulation (where it was verified that locally, even for the larger shear rates $\tau_\gamma > 2 \times 10^2 \tau_s$). The condition $\tau_p \gg \tau_s$ was also verified. As is well known, the timescales relative to shearing and pressure can be combined into a dimensionless number, called the inertial number, which is sometimes used to characterize the flow regimes : $I = \frac{\tau_p}{\tau_\gamma} = \frac{\dot{\gamma}d}{\sqrt{p/\rho}}$. In the concave flow configuration, a global estimate considering all the acceleration values used ($g \sim 10^{-7}$–$10^{-5}\frac{dk_n}{m}$) yields $I_{\text{glob}} = \frac{Vd}{H\sqrt{gH}} = 0.14$–$1.4$ for the range of parameters used in this Letter. Considering the local shear rate (which is, in principle, different from $2V/H$ due to the heterogeneity of the flow), yields a range of local inertial numbers $I_{\text{loc}} = 4 \times 10^{-2}$–$5$, which means that our data are relevant for dense-to-rapid granular flows. Please note that during preparation, the material was subject to a global cumulative deformation of about $\dot{\gamma}\Delta t \sim 10^4$ (locally $> 10^3$). We indeed checked that this is enough to obtain a system at the stationary state.

Inhomogeneous flow profiles. In order to highlight the heterogeneity of the concave flow configuration, we display in Fig. 2 the profiles of average streamwise velocity, granular temperature, and solid fraction. Averages were performed on layers of thickness equal to $1d$, and velocity fluctuations were computed with a correction based on a gradient expansion as in Ref. [27]. The profiles in the figure correspond to a global solid fraction of $\phi \approx 0.55$ and different values of the acceleration g. It is clear that the velocity profile becomes S shaped with increasing g. A zone of higher shear appears, therefore, in the middle of the sample, characterized also by higher
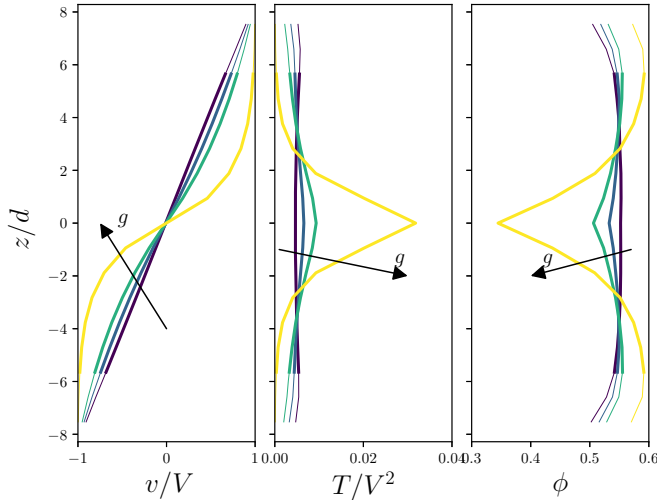
FIG. 2. Average flow profiles in the concave flow, for a global value of solid fraction of $\phi \approx 0.55$ and different values of acceleration g (respectively, $g = 10^{-7}, 10^{-6}, 2 \times 10^{-6}$, and $3 \times 10^{-6} \frac{dk_n}{m}$ when going from dark blue to yellow): (a) streamwise velocity, (b) granular temperature, and (c) solid fraction. The part of the profiles in bold corresponds to data points which were used for the self-diffusion analysis.

granular temperature and lower solid fraction. The central zone becomes, therefore, increasingly collisional and dilute as g increases, whereas, on the other hand, the peripheral zones get denser. Note that above a certain value of g (which depends on the average solid fraction, or N), the peripheral zones become so dense that the central zone is empty of particles. The system is then composed by two separate solid blocks (and is of no more of interest). This sets a limit to the operational range of g. We can conclude that the introduction of a complex force pattern introduces a strong heterogeneity of the kinematic profiles and, particularly, yields gradients of granular temperature. These gradients are strong (i.e., $d\nabla T/T \sim 1$) in the most heterogeneous cases. Granular temperature heterogeneity is often associated with the need of using nonlocal rheologies [28], and the concave flow configuration has been introduced to study such nonlocal effects [26]. The concave flow configuration is also an interesting case for the understanding of how self-diffusivity scalings may be affected by such nonlocal effects.

Self-diffusivity computation. As in previous works, we characterize the self-diffusivity from the trajectories of the particles via the mean squared displacements. For concave flows, given that the flows are inhomogeneous, the analysis is performed on layers one diameter in thickness, normal to z. For each layer, the part of particle trajectories belonging to the layer are considered and averaged to characterize the timescaling of the mean squared displacements via the formula,

$$\langle \Delta x_i \Delta x_j \rangle \propto \Delta t^{\alpha}, \tag{1}$$

where an exponent α close to unity is related to a diffusive behavior. As it was previously shown, for short times $\alpha > 1$ because particle velocity correlations yield a "superdiffusive" behavior. In order to characterize the long-time behavior, we analyze displacements for time lags larger than the correlation

time. In particular, we use an approximation for the correlation time based on granular temperature, and, therefore, we analyze displacements for rescaled time lags $\Delta t \frac{\sqrt{T}}{d} > 1$. On the other hand, the length of the trajectories is not constant (and bounded) because the particles can exit the layers; therefore, for long times there is not enough statistics. The local granular temperature which measures the intensity of fluctuations is relevant in giving a timescale for this problem. We have seen that, in our numerical setup, enough statistics is available for rescaled time lags $\Delta t \frac{\sqrt{T}}{d} < 15$. Within the identified range of time lags, a power law fit permits the verification of the diffusive behavior and the computation of the diffusivity.

Note, however, that the subdivision of the system in thin layers limits the maximum observable displacement in the z direction, which means that the diffusivity components related to that direction [i.e. (zz), (xz), and (yz)] cannot be computed by the method. Details on the timescaling of the mean squared displacements with time is given in Supplemental Material (SM) [29]. Here we limit ourselves to mentioning the main results. First of all, the transverse, (yy), component of the mean squared displacement is clearly diffusive ($\alpha \approx 1$), whereas the mixed (xy) appears to be close to zero. Regarding the streamwise (xx) component in order to compute the displacements, the part of the displacement associated with the shear flow was subtracted from the total displacement in order to avoid considering Taylor dispersion effects.

As detailed in the SM, two types of averaging can be adopted to determine the average shear flow: (i) instantaneous spatial and (ii) time spatial averaging. We find that the type of averaging influences the observed scaling: when subtracting the average velocity profile determined by global time-space averaging, the mean square displacements may display superdiffusive behavior. The observed superdiffusivity is stronger where temperature gradients are larger ($d\nabla T/T \to 1$). On the other hand, using an instantaneous average velocity profile to correct the displacement yields a diffusive behavior.

Given that superdiffusion nearly disappears when changing the definition of fluctuations, it seems reasonable to postulate that its origin has to be found in multiparticle, "eddylike" time correlations which are removed by instantaneous averages. This can be put in relation to the debated concept of "granulence" and the findings of superdiffusion in quasistatic flows [30], and to the concept of granular fluidity, which has been related to velocity fluctuations defined with respect to instantaneous averages [28]. Our results support the idea that it may be important to analyze separately the fluctuations at the scale of a particle from those at the scale of several particles.

Self-diffusion scaling. Based on the above discussion, it is evident that in concave flow, it is possible to evaluate a self-diffusivity coefficient (yy) for the transverse direction, and (xx) for the streamwise direction only when the particle displacements are corrected with the instantaneous spatial velocity gradients. These diffusivities are computed by fitting the mean squared displacement data with the formula,

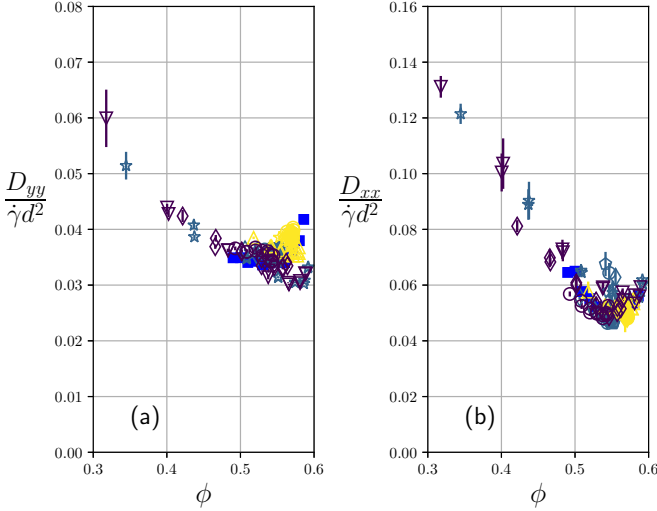$$\langle \Delta x_i^2 \rangle = 2D_{ii}\Delta t. \tag{2}$$

FIG. 3. (a) Transverse (D_{yy}) and (b) streamwise (D_{xx}) self-diffusivities as determined from numerical simulations, scaled by shear rate, vs solid volume fraction. The blue filled squares (■) correspond to homogeneous shearing, and the empty symbols correspond to concave flow. Colors correspond to different average solid fraction values: 0.53 (violet), 0.55 (light blue), 0.57 (yellow), and symbols to different values of $\frac{gm}{dk_n} = 10^{-7}$ (⬡), 10^{-6} (◯), 2×10^{-6} (◇), 3×10^{-6} (▽), 5×10^{-6} (☆), and 10^{-5} (△). Error bars correspond to the 95% confidence interval of the diffusivities determined from the linear fit of the respective averaged mean squared displacement.
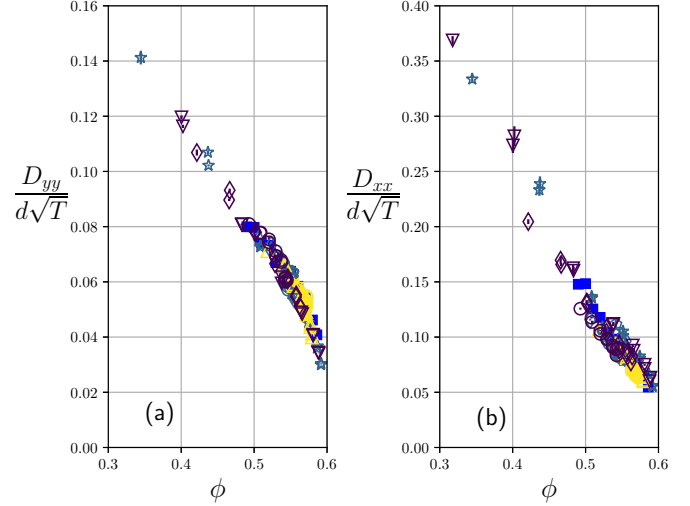

FIG. 4. (a) Transverse (D_{yy}) and (b) streamwise (D_{xx}) self-diffusivities as determined from numerical simulations, scaled by the square root of granular temperature, vs solid volume fraction. The symbols have the same significance as in Fig. 3.

We study scalings of D_{xx} and D_{yy} as a function of system parameters and in comparison to previous homogeneous shear results [13]. Following a scheme discussed in our previous work, we check the relevance of the simplest empirical scaling, based on shear rate; in other words, we study the functions $\frac{D_{ii}}{\dot{\gamma} d^2}$ vs ϕ. These scalings are displayed in Figs. 3(a) and 3(b), where homogeneous shear flow results for D_{xx} and D_{yy} are also reported for comparison. A first general comment is that, in inhomogeneous shear flows, the hierarchy of self-diffusivities is the same as in homogeneous shear ($D_{xx} > D_{yy}$) and, as is well known [11], the self-diffusivities increase (and the difference between D_{xx} and D_{yy} increases as well) when ϕ decreases below 0.5. There is also a global qualitative agreement between homogeneous shear flow and the concave flow results; however, important deviations are evident, particularly, for the more heterogeneous flows (e.g., simulations with large g, denoted by symbols.

Here we limit ourselves to test whether a scaling based on the granular temperature (often associated with "nonlocal" models of granular flows [31,32]) allows better representation of the self-diffusivity results, encompassing also the most heterogeneous simulation data. The scalings $\frac{D_{ii}}{d\sqrt{T}}$ vs ϕ are shown in Figs. 4(a) and 4(b). It is evident that the concave flow data superpose (better here than in Fig. 3) to those of homogeneous shearing. As we showed in our previous work dealing with homogeneous shear flow [13], even in this case the kinetic theory of granular gases [35] underestimates the transverse self-diffusivity by a factor increasing with ϕ and reaching a value of about 3 for denser systems. Nevethe-

less, the physically based self-diffusivity scaling on granular temperature behaves remarkably better than the empirical scaling on the shear rate for both the transverse and the streamwise components, and this is so, particularly, when temperature gradients are important. Our data may, therefore, be used to extend theoretical predictions for the self-diffusivity tensor, which were developed for dilute flows [33,34] to dense systems.

Conclusions. We have measured self-diffusion coefficients in discrete numerical simulations of both homogeneous and inhomogeneous shearing flows of nearly identical frictional and inelastic spheres. The studied systems were relatively dense, i.e., solid fractions from approximately 0.35 to approximately 0.59. In homogenous flows the diffusivity can be estimated by using the grain size d and the inverse of the shear rate $1/\dot{\gamma}$ as, respectively, the natural length and timescales, i.e., $\dot{\gamma}$: $D \propto d^2\dot{\gamma}$. Yet, this purely local scaling does not hold for inhomogeneous flows for which nonlocal effects are important. Here we measured D_{xx} and D_{yy}, i.e., the streamwise and the transverse diffusivities, highlighted their anisotropy ($D_{xx} > D_{yy}$), and showed that the scaling $D_{ii}/d\sqrt{T}$ with T as the granular temperature leads to a better description of the evolution of the transverse diffusivity with the solid fraction than $D_{ii}/\dot{\gamma} d^2$. Besides explaining diffusive properties in inhomogeneous granular shearing flows, this feature could help understanding the nonlocal behavior of granular flows. Our results are, therefore, of immediate interest for researchers working on transport phenomena in dense shearing flows of discrete enties, such as suspensions, traffic flow, crowd dynamics, and active matter.

[1] A. Scott and J. Bridgewater, Powder Technol. **14**, 177 (1976).

[2] H. Buggisch and G. Loffelmann, Chem. Eng. Process.: Process Intensif. **26**, 193 (1989).

[3] S. Savage and R. Dai, Mech. Mater. **16**, 225 (1993), special Issue on Mechanics of Granular Materials.

[4] M. Hunt and S. Hsiau, in *Advances in Micromechanics of Granular Materials*, edited by H. H. Shen, M. Satake, M. Mehrabadi, C. S. Chang, and C. S. Campbell, Studies in Applied Mechanics (Elsevier, Amsterdam, 1992), Vol. 31, pp. 141–150.

[5] V. V. R. Natarajan, M. L. Hunt, and E. D. Taylor, J. Fluid Mech. **304**, 1 (1995).

[6] O. Zik and J. Stavans, Europhys. Lett. **16**, 255 (1991).

[7] Z. S. Khan and S. W. Morris, Phys. Rev. Lett. **94**, 048002 (2005).

[8] N. Taberlet and P. Richard, Phys. Rev. E **73**, 041301 (2006).

[9] J. M. N. T. Gray and C. Ancey, J. Fluid Mech. **678**, 535 (2011).

[10] Y. Fan and K. M. Hill, New J. Phys. **13**, 095009 (2011).

[11] C. S. Campbell, J. Fluid Mech. **348**, 85 (1997).

[12] B. Utter and R. P. Behringer, Phys. Rev. E **69**, 031308 (2004).

[13] R. Artoni, M. Larcher, J. T. Jenkins, and P. Richard, Soft Matter **17**, 2596 (2021).

[14] A. M. Fry, P. B. Umbanhowar, J. M. Ottino, and R. M. Lueptow, AIChE J. **65**, 875 (2019).

[15] R. Cai, H. Xiao, J. Zheng, and Y. Zhao, Phys. Rev. E **99**, 032902 (2019).

[16] M. Macaulay and P. Rognon, J. Fluid Mech. **858**, R2 (2019).

[17] R. Artoni, A. Soligo, J.-M. Paul, and P. Richard, J. Fluid Mech. **849**, 395 (2018).

[18] J. T. Jenkins and F. Mancini, Phys. Fluids **1**, 2050 (1989).

[19] B. O. Arnarson and J. T. Willits, Phys. Fluids **10**, 1324 (1998).

[20] B. O. Arnarson and J. T. Jenkins, Phys. Fluids **16**, 4543 (2004).

[21] M. Larcher and J. T. Jenkins, Phys. Fluids **25**, 113301 (2013).

[22] M. Larcher and J. T. Jenkins, J. Fluid Mech. **782**, 405 (2015).

[23] B. J. Alder and T. E. Wainwright, J. Chem. Phys. **27**, 1208 (1957).

[24] D. Berzi and D. Vescovi, Phys. Fluids **27**, 013302 (2015).

[25] S. Plimpton, J. Comput. Phys. **117**, 1 (1995).

[26] S. Kim and K. Kamrin, Phys. Rev. Lett. **125**, 088002 (2020).

[27] R. Artoni and P. Richard, Phys. Rev. E **91**, 032202 (2015).

[28] Q. Zhang and K. Kamrin, Phys. Rev. Lett. **118**, 058001 (2017).

[29] See Supplemental Material at http://link.aps.org/supplemental/10.1103/PhysRevE.106.L032901 for a discussion on the time scaling of the mean squared displacements with time.

[30] F. Radjai and S. Roux, Phys. Rev. Lett. **89**, 064302 (2002).

[31] D. Berzi and J. T. Jenkins, Soft Matter **11**, 4799 (2015).

[32] D. Berzi, J. T. Jenkins, and P. Richard, J. Fluid Mech. **885**, A27 (2020).

[33] V. Garzó, Phys. Rev. E **66**, 021308 (2002).

[34] M. Abbas, E. Climent, and O. Simonin, Phys. Rev. E **79**, 036313 (2009).

[35] N. V. Brilliantov and T. Poschel, *Kinetic Theory of Granular Gases* (Oxford University Press, Oxford, 2010).